2024-10

Washera Geospace and Radar Science Research Laboratory

Haron, Esleman

COMPARISON OF GEOMAGNETIC STORMS IN SOLAR CYCLES 23 AND 24

WASHERA GEOSPACE AND RADAR SCIENCE RESEARCH LABORATORY

A THESIS SUBMITTED IN PARTIAL FULFILLMENT OF THE REQUIREMENTS FOR THE DEGREE OF MASTER OF SCIENCE IN PHYSICS AT BAHIR DAR UNIVERSITY

BY

Esleman Haron

Advisor: Ambelu Tebabal (PhD)

October, 2024

Bahir Dar, Ethiopia

DECLARATION OF ORIGINALITY

I hereby declare that except where specific reference is made to the work of others, the content of this thesis are original and have not been submitted in whole or in part for consideration for any other degree or qualification in this, or any other university. This thesis work is my own work and contains nothing which is the outcome of work done, except as specified in the text and acknowledgments.

Esleman Haron	_____	_____
Student Name	Signature	Date
Ambelu Tebabal(PhD)	_____	_____
Advisor name	Signature	Date
Tamiru Negussie (PhD)	_____	_____
Head of physics Department	Signature	Date

ADVISOR'S APPROVAL PAGE

To the best of my knowledge and as understood by the student in the research integrity and copyright disclaimer, we examined a thesis entitled "Comparison of geomagnetic storms in solar cycle 23 and 24." by Esleman Haron in partial fulfillment of the requirements for the degree of Master of Science in physics adheres to the provision of guidelines, policies and legislations during his thesis work and use of copyright material. The thesis is completed and can be presented to the thesis evaluation committee

_____	_____	_____
Name of Advisor	Signature	Date (D/M/Y)G.C

Bahir Dar University

College of science

Department of physics

Approval of the project for defense Result

As members of the board of examiners, we examined a thesis entitled “Comparison of geomagnetic storms in solar cycle 23 and 24.” by Esleman Haron in partial fulfillment of the requirements for the degree of Master of Science in physics.

Board examiners

_____	_____	_____
External examiner’s name	Signature	Date
_____	_____	_____
Internal examiner’s name	Signature	Date
_____	_____	_____
Chair person’s name	Signature	Date

Acknowledgements

Blessed be the name of the Lord for guiding my steps in writing this thesis and for most I would like to thank Bahir Dar University for offering me the opportunity to study MSc degree program. Then I would like to give more thanks to my advisor Dr. Ambel Tebabal for his encouragement, guidance, comment and advices during my graduate school carrier. I greatly appreciate him for his constant support, encouragement and friendly relation with me over the past my working time.

Table of Contents

Contents **Page**

List of Table

List of Figures

Acronyms

AU= Astronomical Unit

CMEs = coronal mass ejections

Dst= Disturbance time index

EEJ= Equatorial electrojet

EIA= Equatorial ionosphere anomaly

EUV = Extreme ultra-violate radiation

GI= geomagnetic indices

GMS= geomagnetic storm

GPS= Global positioning system

HMF= heliospheric magnetic field

HSSWS= high sudden solar wind speed

IMF= Interplanetary magnetic field

Kg= kilograms

Km/s = kilometer per seconds

LASCO= LARGE ANGLE AND SPECTROMETRIC CORONOGRAPH

LOS= line of sight

LT= local time

nT= Nino Tesla $=10^{-9}$T

SEP= solar energetic particle

SI= sudden impulse

SOHO = Solar Heliospheric Observatory

SSC= sudden storm commencement

Sws =solar wind speed

UT= Universal time

Abstract

The sun's activity governs the interaction of the magnetosphere with the solar wind and Earth's magnetic field. The influence of the magnetosphere is known as a geomagnetic storm. The main purpose of studying geomagnetic storms is to understand the current passing through the ionosphere. The geomagnetic storms that occurred during solar cycles 23 and 24 were analyzed using the southward interplanetary magnetic field (IMF (Bz)), the interplanetary electric field of the ring current (IEF), the solar wind velocity (SW), and the Dst index from the OMNI data explorer. As the results reveal at the high solar activity, CME-driven geomagnetic storms are more prominent than CIR-driven geomagnetic storms. Moreover, it is clear from the observations of geomagnetic storm events that the occurrence of geomagnetic storms is highly correlated with the southward turning of Bz, the z component of IMF. The magnitude of turning of Bz in a southward direction from a northward direction depends highly upon the severity of the storm. Moderate and intense geomagnetic storms were observed during the years 1996-2019, while they were absent of intense storms during the years 2007-2010. 15 great storms and 7 super storms were observed from 1996 to 2007, while a single great and not super storm were observed during the years 2008 to 2019. The only one great storm was observed in March 17 2015.

CHAPTER ONE

1. INTRODUCTION

1.1 Background of the study

Earth's upper atmosphere plays an important role in ground-based and satellite radio communication and navigation. Above 80 km altitude, the atmosphere contains ionized molecules and free electrons in a region called the thermosphere. Within the thermosphere, the amount of ionized gas becomes appreciable and forms a region called the ionosphere (Moldwin, 2008). The ionosphere is an ionized region of the Earth's upper atmosphere ranging from 60 km to 1000 km in altitude. It comprises a sufficient number of free electrons and positive ions that are electrically neutral and which extends from 50 to 1000 km above the Earth's surface (Rishbeth and Garriott, 1969). The ionization process is mainly due to photons interacting with the atoms and molecules in the ionosphere, which results in the electron being stripped away from the parent atoms and molecules and creating a number of free negatively charged electrons and positively charged ions. The ionospheric F2-layer electron density peak is established essentially as a result of the combined electro of two principal ionospheric processes, loss and diffusion (Brekke and Simmons, 1997). Unfortunately, this layer is also the most anomalous. To contribute to the space weather study, the analysis of the statistical variability of ionosphere parameters is a good means. It is well known that there is a lot of variation in the ionosphere due to the effects of solar, geomagnetic, and meteorological activities. Geomagnetic storms are major disturbances in the Earth's magnetosphere that occur when the interplanetary magnetic field (IMF) turns southward and remains so for a prolonged period of time (Rees, 1994). The reconnection between the southwardly directed component of the solar wind magnetic field, Bz, and the northwardly directed geomagnetic field occurs at the dayside magnetopause, and this reconnection transports energy from the solar wind into the magnetosphere. During a storm, the enhanced ring current is created, and it greatly affects the structure of magnetospheric regions, which in turn results in a significant electric potential on conductors in all kinds of operating systems. As more advanced and interconnected systems are employed, the effects of the upper atmosphere become more profound. Although most operational systems can resist

the effect of certain levels of magnetospheric activity, large storms can still cause significant damage to space- and ground-based installations, such as satellites, long-line communication networks, and electric power grids. Severe geomagnetic storms occur when the IMF imposes for long periods (several hours or more) of the southward component (Bz< 0) with large magnitudes (greater than 10-15 nT). This southward MF stresses the earth's magnetic field, and the degree of this stress, the Dst- index, is the measure of the intensity of the geomagnetic storm. The Dst-index represents the hourly average of the deviations of the horizontal component of the magnetic field measured by many ground stations located between mid and low latitudes. The reference level of Dst is statistically zero on internationally designated quiet days. When the Dst index varies around zero, the geomagnetic field behaves quietly, while Dst greater than or equal to -100 nT means large storms.

In general, the parameters of the solar wind determine the severity of a geomagnetic storm (Burton et al., 1975). Published a formula to predict the Dst index, which uses the velocity and density of the solar wind as well as the Bz-component of the Interplanetary Magnetic Field (IMF) in the Geocentric Solar Magnetospheric System (GSM) as inputs (Gonzalez et al., 1990). Pointed out a relation between the Dst-index and the strength of the IMF, which produced the geomagnetic disturbance: intense storms (Dst -100 nT) were caused by large southwardly directed magnetic fields, where Bz< -10 nT. In addition to this, changes in the Earth's geomagnetic field can cause ionospheric disturbances.

The ionospheric wind dynamo is considered an important and main mechanism in generating electric currents and fields. The disturbed ionospheric wind dynamo can be the generator of the equatorial ionospheric electric currents during geomagnetic storms in the aftermath of strong aurora heating. The magnetospheric electric field directly penetrating into the low-latitude ionosphere can be another source of electric field. During disturbed space weather conditions, magnetospheric electric fields disturb the aurora ionosphere, forming an auroral electrojet, and by the high latitude electric field (E) and thermosphere disturbances can penetrate the equatorial ionosphere. Those are the reasons the equatorial ionospheric electric field variations, like geomagnetic variations, are complex in nature and caused by the superposition of different disturbing agents. The

critical frequency (foF2) at low latitudes was very different in periods when the Bz component turned to the north (the quiet day conditions) and when the Bz component turned south (the main phase of magnetic storms). It is also evident that the solar wind controls not only the auroral ionosphere but also the equatorial ionosphere(You et al., 2009). A geomagnetic storm is a temporary disturbance of the Earth's magnetosphere caused by a solar wind shock wave and a cloud of magnetic field that interacts with the Earth's magnetic field.

The increase in the solar wind pressure initially compresses the magnetosphere. But when the solar wind's magnetic field interacts with the Earth's magnetic field, it transfers increased energy into the magnetosphere. The occurrence of a geomagnetic storm can be varied using different indicators such as Dst-index, AE index, KP-index, and k-index. The Dst-index estimates the globally average change of the horizontal component of the Earth's magnetic field at the equator based on measurements from a few magneto-meter stations, or it is the measure of the magnetic field variation due to equatorial ring currents. The kp-index is an indicator of planetary scope that derives from the k-parameter. The k-index is the quantitative assessment of magnetic disturbance and is calculated with magnet grams (Kelley, 1989.).

During a geomagnetic disturbance, there is an energy input inside the magnetosphere and ionosphere, which changes ionospheric parameters, such as composition, temperature, and circulation. However, during quiet periods, measurements on the ground do not present significant disturbances. Geomagnetic storms are initiated due to the activities of the Sun, mainly by the flares or the coronal mass ejection, when the solar wind velocity, temperature, and density vary drastically, accompanied by significant changes in the north-south component of the interplanetary magnetic field (IMF, Bz) (Mold, 2008).

The Earth has an internal magnetic field generated by the dynamo effects of electric currents in its fluid outer core during quiet periods free of geomagnetic disturbances; the geomagnetic field displays a relatively regular pattern of variation. These regular variations are caused by ionospheric currents generated by the dynamo effect arising from the tidal motion of the thermosphere. The tidal motion of the thermosphere is driven by heat energy from the sun. The Dst values are obtained from the longitudinal average of H variations measured at middle and low-latitude observatories. It is the best indicator

of the ring current intensities and a very sensitive index to represent the degree of solar disturbances. The aim of the statistical study presented in this thesis is to analyze various characteristics of severe geomagnetic storms and their association with different solar interplanetary features for the solar cycles 23 and 24.

Coronal mass ejections (CMEs) are a form of solar activity that causes large interplanetary disturbances, including severe geomagnetic storms and large solar energetic particle events. CMEs originate in closed magnetic field regions, which appear as bipolar or multipolar regions in photospheric magnetograms. Many such magnetic regions contain sunspots, which serve as historical indicators of solar activity. There is usually a good correlation between sunspot number (SSN) and CME rate (Gopalswamy et al., 2010), but the correlation is not perfect because CMEs also originate from non-spot regions such as quiescent filament regions. The drastic reduction in the frequency and magnitude of major geomagnetic storms was attributed to the anomalous expansion of CMEs in cycle 24 (Gopalswamy et al., 2014). They also compared the magnitudes of the southward component of the interplanetary magnetic field that caused major geomagnetic storms in cycles 23 and 24 and found that the Bz values were generally lower in cycle 24.

1.2. Motivation

There are many studies about the overall correlation of solar and interplanetary activity measures with different aspects of geomagnetic activity. Some of the recent analyses are mentioned in the following discussion (Feminella, 1997).Examined the long-term behavior of several solar activity parameters (spots, flares, radio, and X-ray fluxes), confirmed the double peaks, and found that the peaks are more distinct with a clear gap in between when intense and/or long-lasting events are considered. On the other hand, low-energy and short-duration events tend to follow a single-peaked 11-year cycle. The double peaks are reported to be detected in all solar atmospheric layers (photosphere, chromosphere, and corona) up to interplanetary space and are linked with the heliomagnetic cycle. On the other hand,(Kane, 1997) showed that the evolution of various solar indices around sun spot maximum occurs almost simultaneously (within a month or two), and the gap between the two peaks is shown to be sharper for more energetic events. Takalo and Mursula (2020) and Takalo (2020b) have also shown that the

larger the sunspot groups, the more clearly their overall distribution during the solar cycle is double-peaked. And (Le et al. 2013) examined the occurrence of intense storms at the level of−200 nT < Dst ≤− 100 nT, great storms at−300 nT < Dst ≤− 200 nT, and super storms at Dst ≤− 300 nT during the period 1957-2006,based on Dst-indices and smoothed monthly sun spot numbers. We are motivated to see comparisons of geomagnetic storms in solar cycles 23 and 24, and we want to know the various characteristics of the four kinds of geomagnetic storms and the sources of these storms. It is important to understand the complicated current system in the magnetosphere and ionosphere during the storm from the period 1996-2019, based on sunspot number Dst-indices, IMF (Bz), solar wind speed (SWS), and IEF value at the level of Dst <-50nT.

1.3. Objective of the study

1.3.1. General objective

The main objective of this thesis is the comparison of geomagnetic storms in solar cycles 23 and 24.

1.3.2. Specific objective

To investigate the comparison of occurrence rate of geomagnetic storms with disturbed storm time(Dst) index related to the number of sunspot solar wind speed, interplanetary magnetic field(IMF) Bz direction, interplanetary electric field (IEF) in solar cycles 23 and 24.

To examine and achieve a better understanding of geomagnetic conditions during two successive solar cycles.

1.4. The thesis overview

The thesis contains six chapters. The first chapter deals with the background of the research, motivation, and objective of the study. Chapter two describes about, the Earth's atmosphere and ionosphere. Chapter three discusses a geomagnetic storm. Chapter four describes data and methodologies. Chapter five results and discussion, and Chapter six describes conclusion and recommendation.

CHAPTER TWO

2. THE EARTH'S ATMOSPHERE AND IONOSPHERE

2.1. The Earth's Atmosphere

The Earth's atmosphere is the layer of gas, commonly known as air, that surrounds the plant Earth and is retained by Earth's gravity. The atmosphere protects life on Earth by absorbing ultraviolet solar radiation, warming the surface through the heat retention greenhouse effect, and reducing temperature extremes between day and night (Kelley, 1989). The dry air contains 78.09 of nitrogen, 20.95 of oxygen, 0.93 of argon, 0.039 of carbon dioxide, and a small amount of other gas. (Schunk and Nagy, 2009).

2.1.1. Structure of Earth's Atmosphere

The region of the neutral atmosphere is named according to various schemes. The most important classification was based on the temperature altitude profile, which can be described as follows:

The troposphere is the lowest major atmospheric layer, extending from the Earth's surface up to 10 km. In the troposphere, all the Earth's weather occurs; it contains 80 percent of the total mass of the atmosphere. It is characterized by decreases in temperature with height. According to the free encyclopedia, the troposphere is the lowest portion of Earth's atmosphere and contains 75 percent of the atmosphere's mass and 99 percent of water vapor. The end of the troposphere is the tropopause (Davies and Hartmann, 1997).

The stratospheres are the second major atmospheric layer above the troposphere and extend up to 50 km. The stratosphere is characterized by having no weather, an increase in temperature with altitude, and contains over 15 percent of the mass of the atmosphere. Ozone layers also occur in this layer of atmosphere. The upper boundary of the stratosphere is the stratopause (Mohannakumar, 2008).

The mesosphere is the third major atmospheric layer and the middle layer of the atmosphere, and it extends 80–85 km. Mesosphere is characterized by decreasing temperature with increasing altitude, this is due to a decrease in solar heating and an increase in cooling by carbon dioxide radiative emission. It's upper boundary is mesopause, which is the coldest naturally occurring place on the Earth (Arnold, 2007).

The thermosphere is the fourth major layer of the atmosphere and extends about 400-500 km from the mesosphere. It is characterized by increasing temperature with altitude and low air density, and in this layer much of x-ray and UV radiation from the sun is absorbed, and aurora (southern and northern light) occurs as well as charged particles (electron, proton, and ions) from the space collide with atoms and molecules in this layer. The upper boundary is called the thermopause, found at an altitude between 500 and 1000 km (Arnold, 2009).

The exosphere is the uppermost region of Earth's atmosphere as it gradually fades into a vacuum of space. The air on the exosphere is extremely thin, and the reason is the clear upper boundary of the layer because its boundary depends on solar activity.

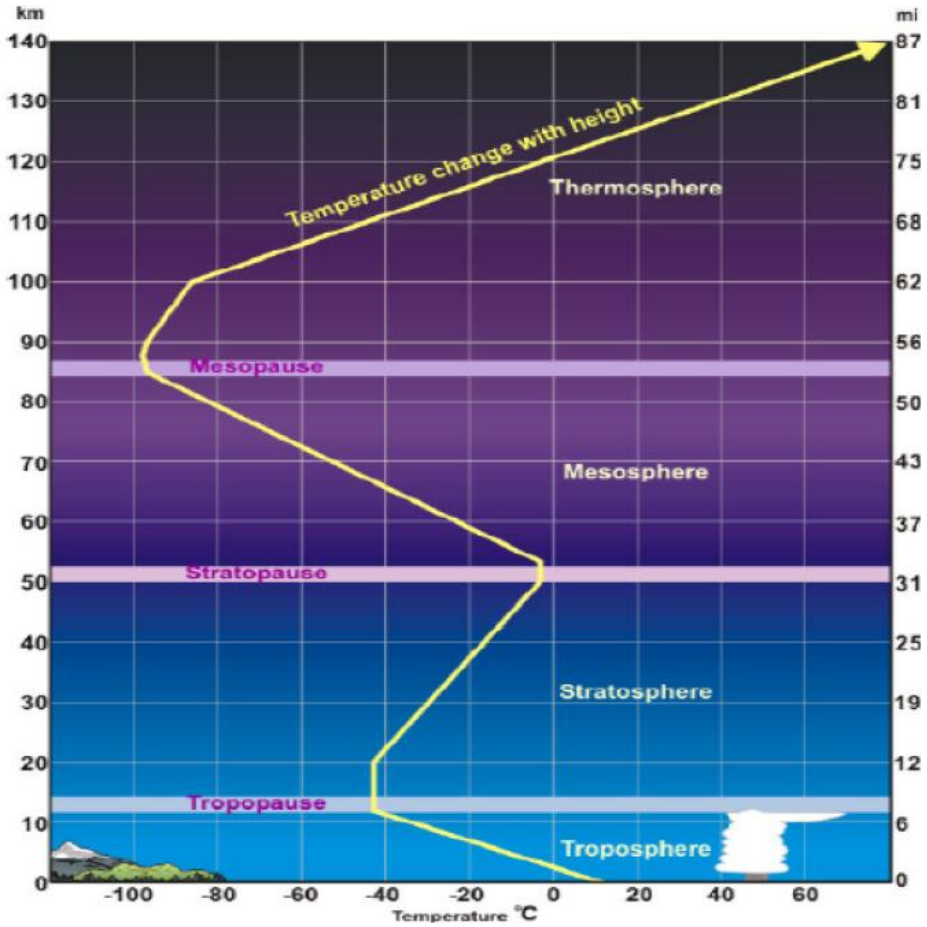

Figure 2.1, a Schematic atmospheric temperature profile, shows the variability of temperature with altitude, and there is considerable variability from one layer to another layer taken from (Okeke and Hamano, 2000)**.**

Fig. 2.1 indicates the vertical structure of Earth's atmosphere with a temperature versus altitude relation. As the figure shows, in the troposphere the temperature decreases as the altitude increases, but in the stratosphere, temperature increases when altitude increases again, and temperature decreases as the altitude increases in the mesosphere. Finally, above the mesosphere, the temperature increases when altitudes increase both in the thermosphere and the exosphere.

2.2. The Earth's Ionosphere

The ionosphere is the part of the atmosphere that contains ionized gases called plasma, and that affects radio propagation. It corresponds to altitudes from 50 to 500 miles at which the atmosphere is so thin that free electrons can exist. The ionization process originates from UV solar radiation and X-ray wavelengths. These photons are energetic enough to dislodge electrons from gas atoms. Simultaneously, those free electrons can be captured by positive ions. This is called recombination. The ratio between ionization and recombination determines the overall electron density. It depends on gas density (at lower altitudes, the combination process accelerates) and on the amount of radiation received from space (sun mainly, but also GRBs). Thus, the ionosphere exhibits a diurnal effect (day/night), a seasonal effect (summer/winter), and a strong relationship with solar activity (11-year sunspot level and solar flares).

Due to the availability of different atoms and molecules with changing rates of absorption, the ionosphere at all latitudes has a tendency to stratify as groups of regions. However, a series of distinct regions or layers of electron density occurred in the daytime ionosphere at mid-latitudes. These layers are denoted by the letters D, E, and F (F1, F2). Each layer is generally characterized by a density maximum at a certain altitude and a density decrease with altitude on both sides of the maximum.

D-Region is the innermost layer from 60 km (37 mi) to 90 km (56 mi) above the surface of the Earth. Ionization here is due to the layman series alpha hydrogen radiation at a wavelength of 121.5 nm ionizing nitric oxide (NO). In addition, high solar activity can generate hard x-rays (wavelength <1 nm) that ionize N2 and O2.

Recombination is high in the D region, net ionization is low, and high-frequency (HF) radio waves are significantly damped within the D region by collision with electrons

(about 10 collisions every millisecond). This is the main reason for the absorption of HF radio waves, particularly at 10 MHz and below; on the other hand, there is progressively smaller absorption at higher frequencies. This effect peaks around noon and is reduced at night due to a decrease in the D-layer's thickness; only a small part remains due to cosmic rays. A common example of the D-layer in action is the disappearance of distant AM broadcast band stations in the daytime (Davies, 1997).

E-Region is the middle layer of the ionosphere from 90 km (56 mi) to 150 km (93 mi) above the surface of the Earth. Ionization is due to the soft x-ray (1-10 nm) and far ultraviolet (UV) solar radiation of ionization of molecular oxygen normally at oblique incidence, and also this layer can only reflect radio waves having a frequency lower than about 10 MHz and may contribute only a little absorption at high frequency. However, during intense sporadic events, the E layer can reflect frequencies up to 50 MHz and higher. The vertical structure of the E layer is primarily determined by the competing effects of ionization and recombination. At night, the E layer weakens because the primary source of ionization is no longer available. After the sun sets, an increase in the height of the E layer maximum increases the range to which radio waves can propagate by reflection from the layer (Davies and Hartmann, 1990).

F-Region, also known as the Appleton Barnett layer, extends from about 150 km to more than 500 km above the surface of Earth (Davies and Hartmann, 1990). It is the densest layer of the ionosphere, which implies signals penetrating this layer will have a charge of escaping into space. At higher altitudes, the number density of oxygen ions decreases, and lighter ions such as hydrogen and helium become dominant. It is the top-side layer of the ionosphere. There is an extreme ultraviolet (UV, 10-100 nm) solar radiation that ionizes the atomic oxygen. The F layer consists of one layer at night, but during the day there are F1 and F2 layers. The F2 layer remains by day and night responsible for most skywave propagation of radio waves, facilitating high-frequency (HF, or short wave) radio communications over long distances. Fig. (2.2) shows the layer of ionosphere from low to higher with different atom and molecule absorption; due to this, the lower ionosphere is the D-region, the next layer of the ionosphere is the E-region, and the upper layer of the ionosphere is called the F-region.

The structure and dynamics of the Earth's upper atmosphere get affected by the intensity of the sun's electromagnetic radiations expelled out due to the variations of solar activity. The Sun's radiations reach the environment of the Earth at all latitudes, and these radiations are the source of various physical processes in the Sun Earth System.

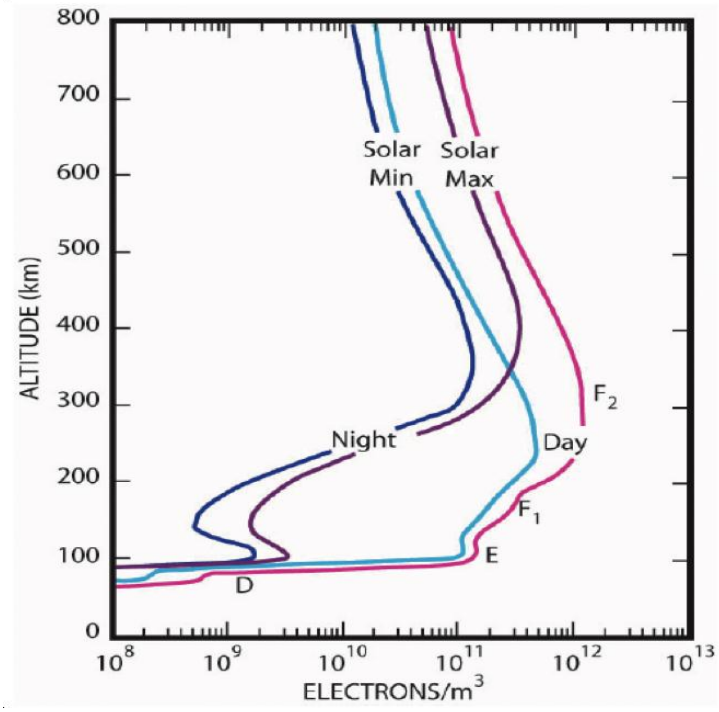

Figure 2.2. Ionosphere adopted from Fayose (2012)

2.3. Space weather

Space weather is the interaction of the sun's atmosphere with the earth's atmosphere. This is affected by the activity of the sun, which makes changes in the number of energetic particles and the plasma in space, which may influence the long-term behavior of the climate on Earth. Space weather is affected by the speed and density of solar wind and IMF driven by solar wind plasma. A variety of physical phenomena are associated with space weather, such as geomagnetic storms, substorms, ionospheric disturbances, scintillation of satellite to ground radio signals, auroras, and geomagnetically induced current on the earth's surface. CMEs and associated shocks, solar energetic particles, and solar flares will also influence the space weather. Some of the space weather effects are: interruptions in the space flight communication, creating satellite drags into low orbits,

radiation sickness to astronauts, power failure in transmission lines, interference in the broadcast of radio, television, and phone signals, interruptions in defense communication, odd behavior in air and marine navigation instruments, altering the atmospheric ozone layer, pipeline corrosion may increase, disrupting global positioning systems, and other spacecraft signals.

2.3.1. Solar flare

A solar flare is defined as the sudden, rapid, and intense brightening over the sun's surface and is interpreted as the sudden release of energy. It emits radiation at all wavelengths, from radio waves to gamma rays in the electromagnetic spectrum. Flares occur in the active regions around the sunspot, where the strength of the magnetic field is stronger. Solar flares were first observed by Richard C. Carrington and Richard Hodgson independently in 1859 and are classified as A, B, C, and M or X flares according to the peak flux. The frequency of occurrence of solar flares depends on the solar cycle, which is more during solar active periods than quiet periods due to the small number of active regions in that period.

2.3.2. Coronal mass ejection (CME)

CMEs (coronal mass ejections) are the mass ejection of matter from the coronal regions of the sun. These CMEs generally occur in large numbers during the period of high solar activity, carrying large numbers of plasmas (= 1023 J and 1013 kg) into the interplanetary medium. The fast (>500 km/s) CMEs coming from the sun into the interplanetary medium are the solar coronal features that contain high magnetic fields. According to Gonzalez et al.'s report, fast CME is a cause of an intense geomagnetic storm (<-100 nT); they consider the effects of interplanetary shock events on the sheath plasma. These high magnetic fields are expected to be capable of interplanetary disturbance. So, coronal mass ejections (CMEs) represent an important source of solar variability from the point of view of plasma and magnetic fields. CMEs remove billions of tons of magnetized plasma from the Sun and dump them into the Sun-Earth connected space once every other day during solar minimum and several times per day during solar maximum.

Geomagnetic activity associated with CMEs can dramatically disrupt electrical and communications systems. CMEs can create voltage surges in electric power grids, disrupt radio communications and navigation systems, prevent normal satellite operations, and

threaten the safety of astronauts (Moldwin, 2008). In 1997, for example, a geomagnetic storm shut down a satellite that provided television broadcasts. In 1998, another storm disrupted a Galaxy IV satellite that supported automated cash machines and airline tracking systems. Geomagnetic storms are also known to affect mobile phone operations and wireless internet services.

2.3.3. The Earth's Magnetic Field and Coronal Mass Ejection

A coronal mass ejection (CME) is an unusually large release of plasma from the solar corona. They often follow solar flares and are normally present during a solar prominence eruption. The plasma is released into the solar wind and can be observed in coronagraph imagery. Coronal mass ejections are often associated with other forms of solar activity, but a broadly accepted theoretical understanding of these relationships has not been established. CMEs most often originate from active regions on the sun's surface, such as groups of sunspots associated with frequent flares. Coronal mass ejections release huge quantities of matter and electromagnetic radiation into space above the sun's surface, either near the corona (sometimes called a solar prominence), farther into the planetary system, or beyond (interplanetary CME). The ejected material is plasma, consisting primarily of electrons and protons. While solar flares are very fast, CMEs are relatively slow. The CME is associated with enormous changes and disturbances in the coronal magnetic field. They are usually observed with a white light coronagraph (Phillips and Tony, 2013).

2.3.4. The impact of coronal mass ejection on Earth

When the ejection is directed towards Earth and reaches as an interplanetary coronal mass ejection (ICME), the shock wave of the traveling mass of solar energetic particles causes a geomagnetic storm that may disrupt Earth's magnetosphere, compressing it on the dayside and extending the nightside magnetic tail.

When the magnetosphere reconnects on the nightside, it releases power on the order of terawatts, which is directed back toward Earth's upper atmosphere. Solar energetic particles can cause particularly strong aurora in large regions around Earth's magnetic poles. These are also known as the Northern Lights (aurora borealis) in the northern hemisphere and the Southern Lights (aurora australis) in the southern hemisphere.

Coronal mass ejections, along with solar flares of other origins, can disrupt radio transmissions and cause magneto-satellite and electrical transmission line facilities, resulting in potentially massive and long-lasting power outages. Energetic protons released by a CME can cause an increase in the number of free electrons in the ionosphere, especially in the high-latitude polar regions. The increase in free electrons can enhance radio-wave absorption, especially in the D-regions of the ionosphere, leading to Polar Cap Absorption (PCA) events. Humans at high altitudes, as in aero planes or space stations, risk exposure to relatively intense cosmic rays. The energy absorbed by astronauts is not reduced by a typical spacecraft shielded sign, and if any protection is provided, it would result from changes in the microscopic homogeneity of the energy absorption event.

2.4. Solar wind

Solar wind is a stream of charged particles such as protons and electrons (plasma) extending outwards from the sun's corona. The stream of particles ejected from the sun was first identified by British astronomer Richard Carrington, and later in 1859, he and Richard Hodgson first observed a sudden ejection of energy from the sun's atmosphere, now called a solar flare. After some days, they observed a geomagnetic storm. A connection between solar wind and comet tail was first suggested by Paul Ahnert, and later Eugene Parker termed it solar wind. Solar wind is divided into two types based on its speed, namely fast solar wind and slow solar wind. Slow solar wind originated from around the sun's equatorial belt called the streamers belt, and fast solar wind originated from 'coronal holes'.

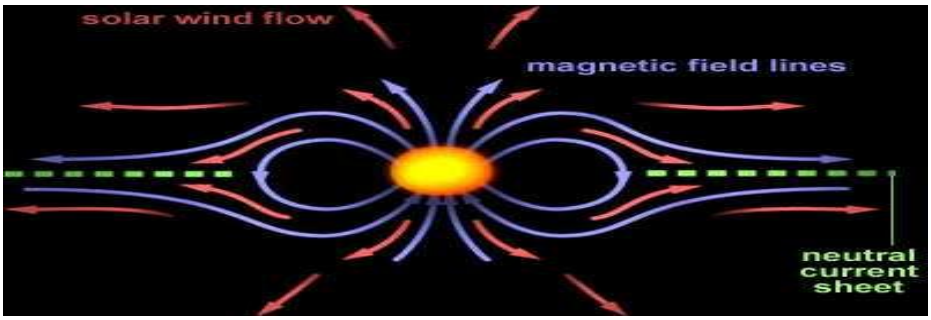

Figure 2.3: The solar magnetic field and IMF seen along the solar equatorial plane adoptedfrom:https://www.google.com/q/density_profile+of_earth_neuteral_atmos

2.5. Interplanetary Magnetic Field

The sun's magnetic field extending into space through solar wind is called the interplanetary magnetic field (IMF). During the solar minimum, the sun's magnetic field resembles that of an iron bar magnet, like Earth's magnetic field with field lines closed at the equator and opened at the poles. Due to the presence of plasma, the sun rotates faster at the equator than at the poles, and this differential rotation makes its magnetic field become twisted, this twisting action creates an 11-year period of solar activity as it reverses its direction about every 11 years. In 1843, Heinrich Schwabe first identified the solar cycle and found that it is cyclical and reaches its maximum around every 9.5 to 11 years. A quantity, which measures the number of sunspots (dark spots on the sun's surface), and groups of sunspots are called the sunspot number, Wolf number, or Zurich number. It was first computed by Wolf in 1848.

The interplanetary magnetic field has three components' Bx, By, and Bz, where Bx and By are parallel to the ecliptic and Bz is perpendicular to the ecliptic. It is a weak field having a strength of about 1 to 37 nT north of earth with an average of 6 nT. The plasma is responsible for the strength of the sun's magnetic field, which is 100 times greater than that of the earth. The solar wind coming towards the earth gets reflected by the earth's magnetic field, which points north at the magnetopause, where the magnetosphere meets the solar wind. But if the IMF points towards south or southward Bz, then the solar wind magnetosphere-ionosphere system strongly depends on IMF, Bz. When the IMF, Bz, is strongly negative, the earth's magnetic field opens its field lines to flow the energy and mass from the solar wind to the magnetosphere. It was first suggested by Dungey (1961). The IMF can control the geomagnetic activity, determining the amount of solar wind energy transfer into the magnetosphere (Arnold, 1971). The intensity of geomagnetic storms varies following the variations of IMF Bz. If the IMF Bz is southward, then reconnection takes place between the IMF field lines and the oppositely directed geomagnetic field lines to enhance the energy transfer (Gonzalez, 1990).

2.6. Earth's magnetic field and co-rotating interaction region

A co-rotating interaction region (CIR) occurs when the fast solar wind streams come from coronal holes and interact with the slow solar wind streams, i.e., the intense

magnetic field can be produced at the interface between the fast and slow streams in the solar wind. When the CIR interacts with the earth's magnetic field, it produces a geomagnetic storm. Co-rotating interaction regions are not always bound by shocks. The reason is that shock formation occurs due to the nonlinear steepening of waves, requiring several nonlinear steepening times to elapse before a shock is formed. Since most CIRs do not have shocks at 1 AU but have steepened into shocks by 2 AU, empirically the nonlinear steepening time must be of order 4 days. The reason why two shocks are eventually formed at a CIR is due to symmetry about the pressure enhancement caused by compression and entraining of the slow wind ahead of the fast stream. (Hofmann-Wellenhof et al., 2001)

2.7. Earth's magnetosphere

The dynamics of the region controlled by the earth's magnetic field is known as the magnetosphere, where the particles are deflected by the Lorentz force. The structure of this region is balanced by the earth's magnetic field, IMF, and solar wind plasma. The solar wind exerts pressure on the earth's magnetic field, by which the magnetosphere gets compressed on the dayside and elongated on the nightside. It ends at the magnetopause, which is about 10 Earth radii from the surface of the earth, where the particles enter into the magnetosphere through partial reconnection of magnetic field lines, and the magnetot ail is 100 Earth radii in length.

The imaginary surface at which the solar wind is first deflected is called the bow shock. The variation of the distance between the bow shock and the Earth depends on the strength of the solar wind flow. The corresponding region behind the bow shock and surrounding the earth is termed the magnetosphere, the region dominated by the earth's magnetic field, which prevents the solar wind from entering. When the solar wind (plasma) enters the bow shock, its density, temperature, and magnetic field increase, while its velocity decreases.

The region between the bow shock and magnetopause, dominated by the sun's magnetis m, is called the magneto sheath and contains compressed and heated solar wind plasma.

The magnetopause is the boundary at which the magnetosphere ends on the sun-ward side of the earth, where the solar wind interacts with the magnetosphere.

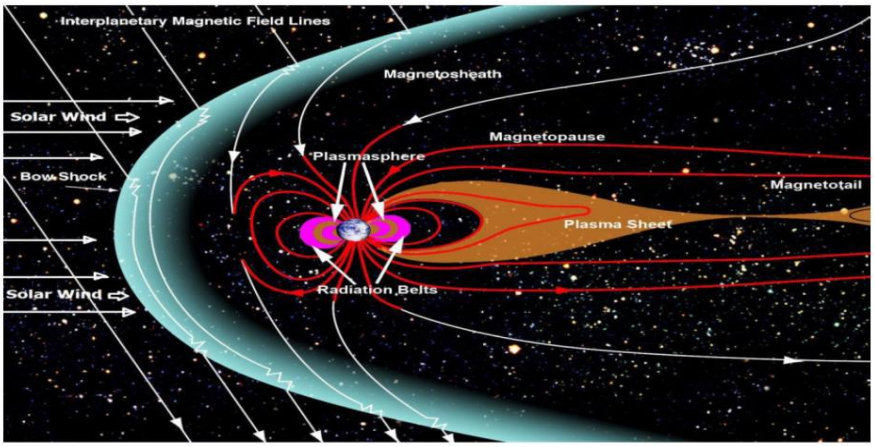

Figure 2.4: the solar wind speed and magnetic field interaction adopted from Aaron Kaase/ NASA/Goddard.

The magnetotail is the area on the nightside of the earth formed by the pressure from the solar wind, which pushes the earth's sunward field inwards and drags the nightside out into a tail more than a million kilometers long. Most of the solar wind particles that hit the magnetopause are deflected and swept back in to the magnetotail, while the ones that penetrate become part of the energetic Van Allen radiation belts

Earth's magnetic field exerts a force on moving electrical charges and can trap the particles in a region called the Van Allen radiation belt. The equatorial current sheet separates the magnetotail into two regions called the lobes and flows from dawn to dusk. The magnetic field in the north lobe is directed away from the earth, whereas the magnetic field in the south lobe is directed towards the earth. Plasma density is very low in this area. The plasma sheet is found between the lobes in the magnetotail and contains extremely hot ions and electrons. The plasma sphere is the area around the earth where cold plasma co-rotates with the earth, where the geomagnetic field is dominated. It is located above the ionosphere, and its outer boundary is the plasmapause.

2.8. Magnetic Reconnection

The phenomenon of magnetic reconnection is responsible for the magnetospheric flows and the dynamics of the solar corona. Reconnection was first applied to magnetospheric physics by Dungy, in 1961. Magnetic reconnection is defined as the breaking and reconnecting of magnetic field lines, which are oppositely directed, in plasma. Here magnetic field energy is converted to plasma kinetic and thermal energy.

Reconnections are possible at two points in the earth's magnetosphere. The first point of reconnection in the Earth-Sun system occurs at the magnetopause, where the solar wind (carrying IMF) interacts with the Earth's magnetic field and produces an open path through which it exchanges mass, energy, and momentum to the sunward side of the magnetosphere. The earth always has a northward topology due to its dipole configuration, but the solar wind switches between southward and northward, and so this reconnection only happens when the solar wind has a southward component.

A second reconnection point occurs in the magneto tail at the neutral point, which allows plasma to flow from the magnetospheric currents back into the solar wind and away from the earth to re-establish the equilibrium of the system. The long stretched field of the magneto tail becomes unstable and rearranges to form two regions, one controlled by the earth's field and the other one that is part of the solar wind again.

CHAPTER THREE

3. GEOMAGNETIC STORM

A geomagnetic storm is a temporary disturbance of the earth's magnetosphere caused by a solar wind shock wave and cloud of the magnetic field that interacts with the earth's magnetic field. The increases in the solar wind pressure initially compressed the magnetosphere. The solar wind's magnetic field interacts with the earth's magnetic field and transfers an increase in energy to the magnetosphere (Gummow, 2002). Both interactions cause an increase in the plasma movement through the magnetosphere (driven by increased electric fields in the magnetosphere) and an increase in the electric current in the magnetosphere and the ionosphere. Several space weather phenomena tend to be associated with geometric storms or caused by geomagnetic storms. This includes solar energetic particle (SEP) events, geomagnetically induced current (GIC), ionospheric disturbances that cause radio and radar scintillation, disruption of navigation by magnetic compass, and auroral displays at much lower latitude than normal.

A geomagnetic storm is also defined by changes in the disturbance storm time index (Dst). The Dst index estimates the globally averaged change of the horizontal component of the earth's magnetic field at the magnetic equator based on measurements from a few magnetometer stations. Dst is computed once per hour and reported in near real-time; during quiet time, the Dst is between -20 and +20 nT. (Brekke and Simmons,1997).

3.1. Types of Geomagnetic Storms

There are two main types of geomagnetic storms: recurrent and nonrecurrent storms. Recurrent storms are caused by features on the sun called coronal holes that live for several months and generate Corotating interaction regions (disturbances in the solar wind where the fast solar wind from the coronal holes catches up with the slow solar wind) that repeat on the 27-day solar rotation period, and Nonrecurrent storms occur sporadically throughout the solar rotation but are primarily driven by CMEs. Co-rotating interaction regions are most commonly observed during the declining phase of the solar cycle (the few years after the solar maximum) into the solar minimum, whereas CMEs are seen most of the tendering solar maximum.

3.2. Phase of Geomagnetic Storm

There are three phases of geomagnetic storms, namely the initial, main, and recovery phases. Initial phases are characterized by Dst (it is a one-minute component of SYm-H) increasing by 20 to 50 nT intense per minute. It is referred to as a storm sudden commencement (SSC). However, not all geomagnetic storms have an initial phase, and not all sudden increases in Dst or SYm-H are followed by a geomagnetic storm. The main phase of a geomagnetic storm defined by Dst decreasing to less than (<-50 nT) to define a storm is somewhat arbitrary; the minimum value during a storm will be between -50 and approximately -600 nT. The duration of the main phase is typically 2-8 hours. During the main phase of a geomagnetic storm, electric current in the magnetosphere creates a magnetic force that pushes out the magnetosphere and solar wind. The recovery phase is defined by the Dst-index; it changes from the minimum value to the quite time value. The recovery phase may last as short as 8 hours or as long as 7 days.

3.3. Formation and Measurement of Geomagnetic Storm

Geomagnetic storms are triggered by an increase in the plasma density and the speed of the solar wind after a solar flare or an earthward-directed CME. These increases raise the pressure of the solar wind in the magnetopause and deform the magnetosphere. On the daytime side, the magnetopause approaches our planet along the Sun-Earth line, moving from 11 Earth radii to only 4-5. At the same time, the region corresponding to the nighttime hemisphere stretches out in a very complex manner, similar to a tube of tooth paste squeezed in the middle. This intensifies the earth's magnetic field and increases its bow-wave pressure against the solar wind, reaching a new equilibrium position. All these phenomena give rise to the geomagnetic storm, which affects, to a lesser or greater extent, the whole planet. Depending on the speed of the disturbed solar wind, it will occur between one and four days after the violent event on the surface of the sun.

3.4. Historical occurrence of Geomagnetic Storm

The first observation of the effects of geomagnetic storms occurs early in the 19th century, from May 1806 until June 1807 in Germany (Alexander von Humboldt) recorded the bearing of a magnetic compass in Berlin (Russell and Randy 2010). The second geomagnetic storm occurred on September 1 to 2, 1859. From August 28 until September 2, 1859, numerous sunspots and solar flares were observed on the sun, with

the largest flare on September 1. It can be assumed that a massive CME was launched from the sun and reached the Earth within 18 hours. That takes normally 3 to 4 days. The horizontal field was reduced by 1600 nT as recorded at Coolabah observatory, and it is estimated to be approximately -1760 nT (Brekke, 1997).

The disruption of telegraph service and initiation of fires was observed; an aurora of November 17, 1882, and May 1921 and 1960, common radio disruption, was reported. The March 1989 geomagnetic storm caused the collapse of the hydro-Quebec power grid in seconds as the equipment protection relay stripped in a cascading sequence. Six million people were left without power for nine hours. The storm causing this event was the result of a coronal mass ejected from the sun (extreme space weather events national Geophysics data center).

The minimum of the Dst-index value was -589 nT. On March 14, 1989, an x5-class flare erupted known as the Bastille Day event, and a coronal mass was launched directly at earth. Generally, during a geomagnetic storm, the ionosphere's F2 layer becomes unstable, fragments, and may disappear. In the north and southern pole regions of the earth, auroras are observable.

3.5. Effects of Geomagnetic Storm

There are many effects of a geomagnetic storm; these include radiation hazards to humans, disruption of electrical systems, communications, navigation systems, satellite hardware damage, mains electrical grid, geologic exploration and pipelines, etc. Radiation hazards to humans: this effect of a geomagnetic storm exists when an intense solar flare releases very high-energy particles that have a tendency to produce radiation that will poison humans and other mammals; this effect is generally similar to low-energy radiation from a nuclear blast. The earth's atmosphere and magnetosphere allow adequate protection at ground level, but astronauts are subject to potentially dangerous doses of radiation.

The penetration of high-energy particles into living cells can cause chromosome damage, cancer, and other health problems. Solar protons with energies greater than 30 MeV are particularly hazardous. Solar proton events can also produce elevated radiation from aircraft flying at high altitudes. Although these risks are small, monitoring of solar proton events by satellite instrumentation allows the exposure to be monitored, and evaluated,

and eventually flight paths and altitudes adjusted in order to lower the absorbed dose of the flight (Scott, 2007). Disruption of the electrical system: it has been suggested that a geomagnetic storm on the scale of the solar storm of 1859 would cause billions of dollars of damage to satellites, power grids, and radio communications and could cause an electrical blackout on a massive scale that might not be repaired for weeks (Kelley, 1989).

Communication: many communications systems use the ionosphere to reflect radio signals over very long distances. Ionospheric storms can affect radio communication at all latitudes. Some frequencies are absorbed and others are reflected, leading to rapidly fluctuating signals and unexpected propagation paths. TV and commercial radio stations are little affected by solar activity, but ground to air, ship to shore, short wave broadcast, and amateur radio (mostly the bands below 30 MHz) are frequently disrupted. Radio operators using the HF band surely rely upon solar and geomagnetic alerts to keep their communication circuit-up and running. Some military detection or early warning systems are affected by solar activity. The over-horizon radar bounces signals off the ionosphere to monitor the launch of aircraft and missiles from long distances. During a geomagnetic storm, this system can be severely hammered by radio clutter. Some submarine detection systems use the magnetic signatures of submarines as one input to their locating schemes (Hargreaves, 1992). Geomagnetic storm scans mask and distort these signals, and also telegraph lines in the past were affected by geomagnetic storms.

Navigation Systems such as GPS (global positioning systems), LORAN (long-range navigation), and the new defunct OMEGA are adversely affected when solar activity disrupts their signal propagation. The omega system consists of eight transmitters located throughout the world. Airplanes and ships used the very low-frequency signals from these transmitters to determine their positions. During solar events and geomagnetic storms, the system gave navigators' information that was accurate by as much as several miles. If navigators had been alerted that a proton event or geomagnetic storm was in progress, they could have switched to a backup system.

GPS signals are affected when solar activity causes sudden variations in the density of the ionosphere, causing the GPS signals to scintillate (Scott, 2007). Satellite hardware damage, the geomagnetic storm, and an increase in the solar ultraviolet emission heat the

earth's upper atmosphere, causing it to expand. The heated air rises; and the density at the orbit of the satellite up to about 1000 km (621 mi) increases significantly. This results in increased drag, causing satellites to slow and change orbits lightly.

Another problem for satellite operators is differential charging; during a geomagnetic storm, the number and energy of the electrons and ions increase. When a satellite travels through this energized environment, the charged particles striking the spacecraft differentially charge portions of the spacecraft. Discharges can cross spacecraft components, harming and possibly disabling them. Buck changing, also called deep charging, occurs when energetic particles, primarily electrons, penetrate the outer covering of a satellite and deposit their charge in its internal parts. If sufficient charge accumulates in any one component, it may attempt to neutralize by discharging to another component. This discharge is potentially hazardous to the satellite and the satellite's electronic system (Kelley, 1989).

In the main electrical grid, when magnetic fields move about in the vicinity of a conductor such as a wire, a geomagnetically induced current is produced in the conductor; this happens on a grand scale during geomagnetic storms (the same mechanis m also influenced telephone and telegraph lines before fibre optics) for all long transmissi on lines (Kelley, 1989).

In geologic exploration, the earth's magnetic field is used by a geologist to determine subterranean rock structures. Geometric surveyors are searching for oil, gas, or mineral deposits. They can accomplish this only when the earth's field is quiet, so that true magnetic signatures can be detected. Other geophysicists prefer to work during geomagnetic storms. When strong variation in the earth's normal surface electric currents allows them to stimulate subsurface oil or mineral structures.

This technique is called magnetotellurics. For these reasons, many surveyors use geomagnetic alerts and predictions to schedule their mapping activities.

Pipelines and rapidly fluctuating geomagnetic fields can produce geomagnetically induced currents (GIC) in pipelines. This can cause multiple problems for pipeline engineers. Pipeline flow meters can transmit erroneous flow information, and the corrosion rate of the pipeline is dramatically increased. If engineers incorrectly attempt to balance the current during a geomagnetic storm, corrosion rates may increase, even

pipeline managers, thus receiving space weather alerts and wrappings to allow them to implement defensive measures (Scott, 2007).

3.6. Risk assessment for the effect of geomagnetic storm

There are many ways of risk assessment for the effect of a geomagnetic storm; these are using emergency supplies, preparing for power surges, and unplugging electronic devices. Emergency supplies are used to protect the effect of a geomagnetic storm by creating an emergency for all, such as flash lights, batteries, cooking and heating fuel food, as well as clean water. Also consider a backup stash with paper copies of finance and personal records, cash, a roadmap address book, a radio, a first aid kit, and something else you need if your handy digital gizmos along with your car, credit cards, bank, and shopping center are out of commission for a while (Rishbeth, 1969). Preparing for power surges can be either whole-house surge protectors or individual surge protectors. Whole-house surge protectors are connected to your breaker panel and provide protection from lighting and other power surges, whereas individual surge protectors are used in the absence of whole-house surge protectors to install surge protectors on computers, TVs, stereos, and other electronics (Rishbeth, 1969).

CHAPTER FOUR

4. DATA AND METHODOLOGIES

4.1. Data Source

The solar wind speed, interplanetary magnetic field (IMF), and Dst (disturbance time index) data were taken from Omni Web Data Explorer (http://Omniweb.gsfc.nasa.gov/). In addition to these, the data for the sunspot number has been taken from the solar influence data center in Belgium, following the website http://sidc.oma.be/silso/datafiles.

4.2. Method of analysis

Based on the data obtained, the graph that shows the peak values of the solar and geomagnetic parameters has been plotted using MATLAB. We have studied the solar and geomagnetic conditions during 1996–2007 of solar cycle 23 and the years 2008–2019 of solar cycle 24 and have presented the comparative result; specifically, we have carried out the comparison of the sunspot number. We have also studied 566 cases of geomagnetic storms (Dst <-50 nT) that occurred from 1996 to 2007 and 266 cases of geomagnetic storms (Dst <-50 nT) that occurred from 2008 to 2019.

The data used in this thesis to study the comparison of geomagnetic storms during solar cycles 23 and 24 is obtained from the OMNI data explorer. These data contain the interplanetary magnetic field (IMF (Bz)), Dst-index, the solar wind (plasma) speed, and the interplanetary electric field IEF (Ey), which is linked tohttp://omniweb.gsfc.gov/form/dx1.html. To be used, the OMNI data explorer first assigns the geomagnetic storm by using the DST-index value. The geomagnetic storms are classified into three; based on the DST-index value, these are weak. Dst-index value -30 nT > DST > -50 nT, moderate storm Dst-index value -50 nT > Dst>-100nT and an intense storm Dst-index value <-100nT, in addition to this, if it's Dst-index value < -200nT, is called an extreme storm, and Dst-index value <-500nT is called a super storm (Brekke, 1997).

The data for the Dst-index value could be downloaded from the Geomagnetic Equatorial Dst-index home page (htt://wdc.kugi.kyoto-u.ac.jp/dstdir). The Dst-index value quite day is between -20 nT and 20 nT. The interplanetary magnetic field (IMF) value can be

determined by the Bt-value, and the Bt-value of IMF indicates the total strength of IMF, i.e., the higher the value, the better the condition for an enhanced geomagnetic storm.

The IMF is a vector and has three axis components: Bx, By and Bz. But the two components (B_x and By) are parallel to the elliptic due to this. It has no auroral activity effects, whereas the third (Bz) is perpendicular to the elliptic and is created by the wave and disturbance storm. Because the IMF (Bz) has a geomagnetic storm when it turns either northward or southward. When the IMF (Bz) moves in a southward direction and interacts with the northward direction of the Earth's magnetic field, i.e., it attracts each other and causes the disturbance geomagnetic storm: this disturbance occurs when the charged particle has easier time to enter the magnetosphere.

CHAPTER FIVE

5. RESULTS AND DISCUSSIONS

In this chapter, we are going to analyze the occurrence rate of geomagnetic storms with (Dst <-50 nT) and yearly mean sunspot number during solar cycles 23 and 24. We have also analyzed different events of geomagnetic storms during 1996 to 2019 related to its DST index, IMF (Bz), IEF, and SWS. The result is analyzed first, and then discussion will be followed.

5.1. Occurrence rate of geomagnetic storm and sunspot number

A geomagnetic storm is a major disturbance of Earth's magnetosphere due to the interaction of a southward interplanetary magnetic field with the earth's magnetic field. The interaction leads to induced additional energy to the magnetotail of the magnetosphere. These energies lead to varying dispersion of the earth's magnetic field to some extent. The variation of the earth's magnetic field is considered to be a geomagnetic storm.

Table 5.1 shows that the number of geomagnetic storms (Dst < -50 nT) was more significant during solar cycle 23 compared to solar cycle 24. These observations are in agreement with several studies (Echer et al., 2008) where, comparing the rising phases of solar cycles 23 and 24, it is shown that there were 46 moderate storms, 4 intense storms and no great and super storms in the first 4 years of the cycle 24, compared to 136 moderate storms, 25 intense storms, 3 great storms and no super storm during the same period of cycle 23. Based on a detailed statistical study of geomagnetic storms (Dst < −100 nT) of solar cycle 23 (Gonzalez et al., 2007), they have reported on intense storms and their associated solar sources and showed that the most common structures leading to the development of an intense storm are magnetic clouds (MC), coronal mass ejection (CMEs), and high-speed solar wind. The drop in these solar plasma conditions leads to a calm geomagnetic condition on Earth. Then, it appears that solar cycle 23 was most disturbed with important input energy into Earth's atmosphere compared to solar cycle 24. Table 5.1 lists the number of storms (moderate, strong, severe, and great) observed year-wise during the years 1996–2019. In total, 390 moderate, 154 intense, 15 great, and

7 super storms were observed from 1996 to 2007, while during the years 2008–2019, only 231 moderate, 34 intense, and one great storm were observed.

Year	Moderate -100nT < Dst-≤-50 nT	Intense -200 < Dst ≤ -100nT	Great -300 nT < Dst ≤ -200nT	Super Dst ≤ -300 nT	Yearly mean sunspot number
1996	14	1	---	---	12
1997	34	5	---	---	29
1998	46	12	2	---	88
1999	42	7	1	---	136
2000	50	13	6	---	174
2001	41	17	5	1	170
2002	32	18	---	---	164
2003	39	6	---	5	99
2004	25	9	1	1	65
2005	39	11	---	---	46
2006	23	1	---	---	25
2007	5	---	---	---	13
2008	5	---	---	---	4
2009	1	---	---	---	5
2010	16	---	---	---	25
2011	24	4	---	---	81
2012	35	8	---	---	85
2013	30	3	---	---	94
2014	27	1	---	---	113
2015	38	11	1	---	70
2016	31	4	---	---	40
2017	14	2	---	---	22
2018	6	1	---	---	7
2019	4	---	---	---	4

Table 5.1.Annual occurrence rate of geomagnetic storms with Dst index values <-50 nT, and yearly mean sunspot number during solar cycles 23 and 24 (1996-2019).

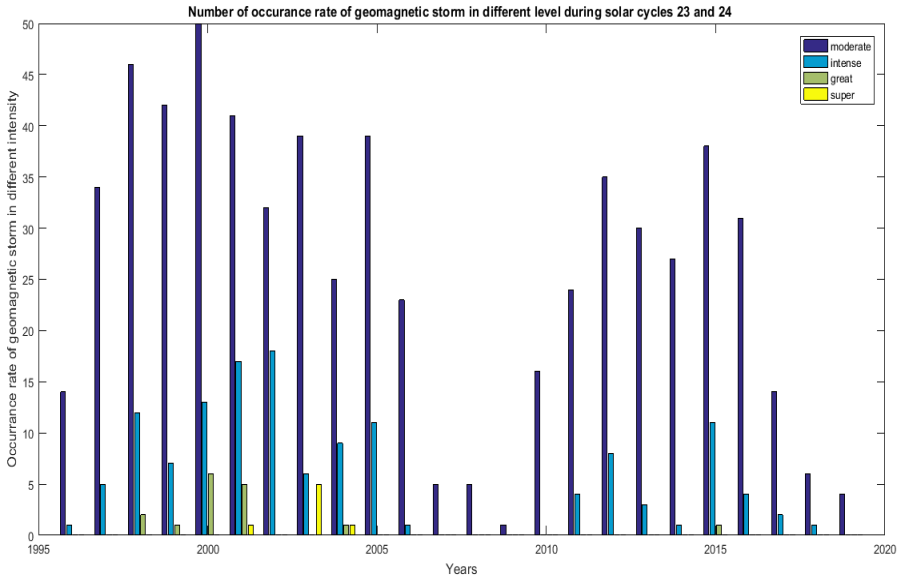

Figure 5.1.Number of geomagnetic storms of different levels between 1996 and 2019.

The numbers of geomagnetic storms of various categories have been shown in Figure 5.1. He found that moderate and intense geomagnetic storms were observed between 1996 and 2019. However, absent of intense storm during the years 2007 and 2010. 15 great storms and 6 super storms were observed between 1996 and 2007, with only one great storm and no super storms observed. Between the years 2008 and 2019, the only great storm observed was in 2015. Halo CMEs are responsible for high geomagnetic conditions (Gopalswamy et al., 2007). This means that when fewer numbers of halo CMEs are observed, there will be a minimal number of geomagnetic storms. Based on Figures.5.2 and 5.3, we conclude that solar and geomagnetic activities were less during the first six years of solar cycle 24 as compared to solar cycle 23.

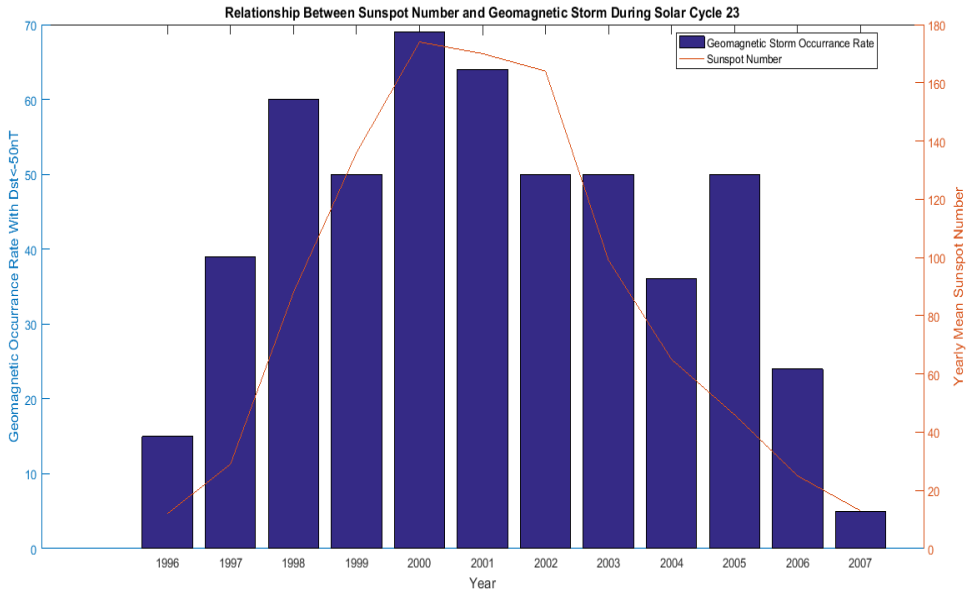

Figure 5.2: Number of storms with the average annual number of sunspots between1996 and 2007(solar cycle 23)

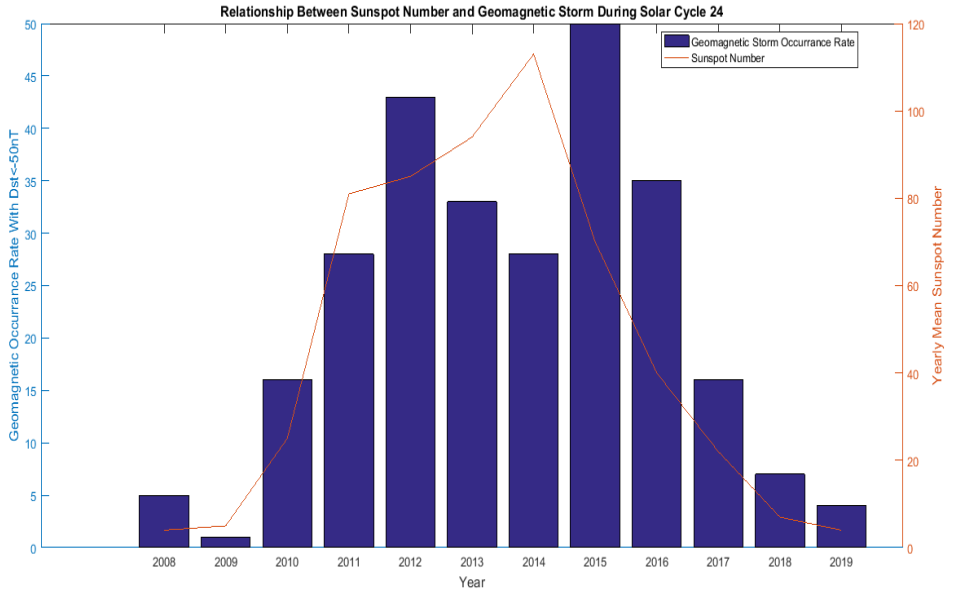

Figure 5.3 Number of storms with the average annual number of sunspots between 2008 and 2019(solar cycle 24).

The low activity during solar cycle 24 is linked to several parameters, such as the low solar wind pressure after the solar minimum that followed solar cycle 23, the low sunspot

number, the low number of intense geomagnetic storms, and the length of the deep minimum that followed solar cycle 23. The fluctuation observed in all the aforementione d indices indicates the level of geomagnetic disturbances and the drop in the amplitude of the solar and geomagnetic parameters from solar cycle 23 to solar cycle 24, which is characterized by magnetically weak conditions. Another characteristic of the solar cycles 23 and 24 is the occurrence of the sunspot number: The sunspot number has been a very useful indicator of solar activity level.

In Figures. 5.2 and 5.3, we have shown the variation of sunspot numbers for the years 1996 to 2007 and 2008 to 2019 with relation to the number of geomagnetic storms. The maximum of the sunspot number during solar cycle 24 was 113 and occurred in April 2014, when the maximum of solar cycle 23 was extended over a period of four years (1999-2002) with a peak of 174 sunspots obtained during the year 2000.

5.2. Event 1: The Geomagnetic Storm of July 14-18, 2000.

Fig.5.4 represents plots of Dst index top panel, interplanetary magnetic field IMF (Bz) upper middle panel, interplanetary electric field (IEF) lower middle panel, and solar wind speed (SWS) bottom panel for five consecutive days from the 14^{th} to the 18th of 2000.

Between July 14 and July 18, 2000, a significant geomagnetic storm occurred, driven by intense solar activity. This event was characterized by variations in several key parameters: the Dst index, interplanetary magnetic field (IMF) Bz component, interplanetary electric field (IEF), and solar wind speed. On day 14 around 24:00 UT, quiet storms about -29 nT, the geomagnetic storm began to intensify as the CME, which had been released from the Sun a few days earlier, made contact with Earth's magnetic field. On day 15 at 21:00 UT initial signs of increased solar wind speed and southward Bz values were recorded, followed by another great storm reaching -289 nT. On day 16 at 24:00 UT, an interplanetary shock was driven by the magnetic cloud, it caused a super storm fall in the Dst index, reaching its minimum of -300 nT. The storm reached its peak intensity. The Dst index dropped sharply to around -300 nT, indicating a strong magnetic disturbance. The low Dst values indicated that the storm was significant, with the potential for disruptions in power grids and satellite operations. At the main phase time, the IMF (Bz) is southward lading, intensifying the ring current. The Bz component was predominantly southward during the storm period, this persistent southward orientation

allowed for continuous magnetic reconnection and enhanced geomagnetic activity, and IEF is the northward. The IEF of the ring current at time of sudden commencement decreases, but during the main storm it starts increasing nearly to 45V/m at 3:00 UT. The IEF elevated values contributed to the enhanced electric fields in the magnetosphere, driving geomagnetic currents and leading to observable phenomena like auroras. Speeds reached up to 800 km/s, a considerable increase compared to normal solar wind conditions. The increased solar wind speed provided additional energy and momentum to the geomagnetic processes, intensifying the storm effects. 17-18 continued geomagnetic activity Dst recovery. The IMF remained predominantly southward, and moderate geomagnetic activity continued, with Dst values fluctuating but remaining negative. Solar wind speeds began to decrease gradually which typically hover around 600 km/s.

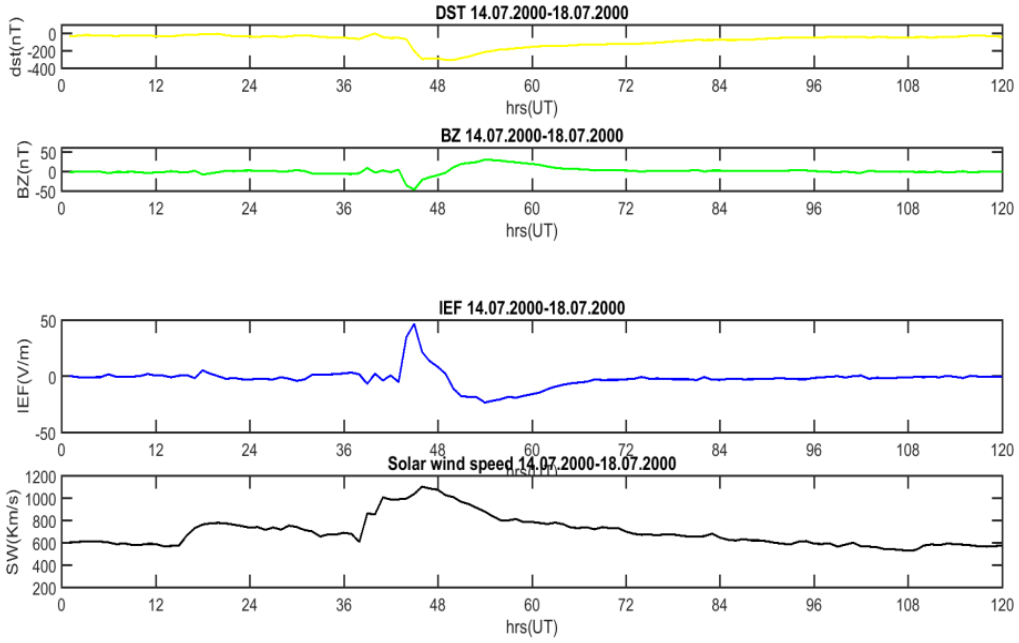

Figure 5.4 Dst index (top panel), IMF, Bz (upper middle panel), Solar wind speed (bottom panel), IEF (lower middle panel) during July 14-18 2000

The storm's impacts gradually waned, but elevated levels of geomagnetic activity persisted, with occasional high IEF values. This storm took about 31 hours to reach its normal Dst value.

The geomagnetic storm that occurred from July 14 to 18, 2000, was a significant space weather event caused by a coronal mass ejection (CME) that impacted Earth's magnetosphere, was marked by low Dst index readings, a southward IMF Bz component, high IEF values, and increased solar wind speed. These factors combined to create a significant and impactful geomagnetic storm, influencing Earth's magnetosphere and space weather conditions during this period.

5.3. Event 2: The Geomagnetic Storm of November, 6-10, 2004.

Fig. 5.5 shows plots of disturbance storm time (Dst) index top panel, interplanetary magnetic field (IMF (Bz)) (upper middle panel), solar wind interplanetary electric field (IEF) (lower middle panel), and speed (SWS) (bottom panel) for five consecutive days from day 6th to 10^{th} November 2004. As shown in Fig (5.5), November 6-7 Initial decrease in Dst index to around -50 to -100 nT, indicating early storm onset. The Bz component began to show southward orientation, which is a precursor to geomagnetic storm conditions. Elevated IEF values began to emerge as a result of increasing solar wind speed and IMF strength. Solar-wind speeds began to increase, reaching levels above 500 km/s.

However, November 8: Reached a minimum of around -374 nT, reflecting a strong and intense ring current. This level of Dst indicates high energy input from the solar wind, significant magnetic activity, and the great storm. This deep decline in the Dst index indicates a robust ring current and significant energy input into the magnetosphere. The Bz component was consistently negative, with prolonged periods of southward orientation. This sustained southward Bz was crucial for driving the intensity of the geomagnetic storm. The IEF reached high levels, reflecting strong solar wind magnetosphere interactions. Elevated IEF contributes to increased geomagnetic activity and storm intensity. Solar wind speeds peaked around 700 km/s, contributing to the heightened geomagnetic activity.

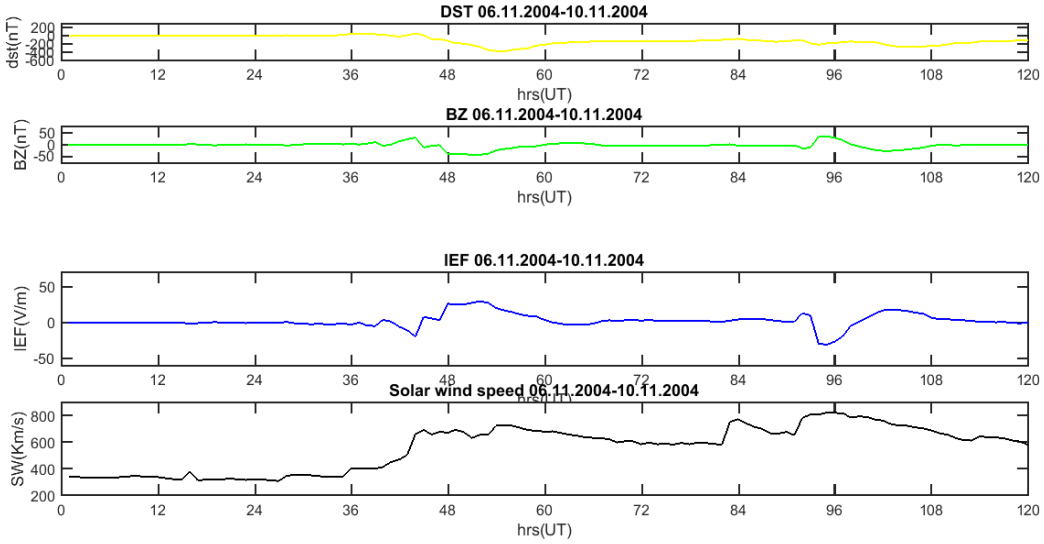

Figure 5.5.Dst index (top panel), IMF, Bz (upper middle panel), Solar wind speed (bottom panel), IEF (lower middle panel) during November 6-10 2004.

November 9-10: The storm's intensity began to subside, with a gradual recovery of Dst indices. While geomagnetic activity remained high, the levels of disturbance started to diminish. The Bz component gradually returned to more neutral or northward values, signalling a decrease in storm intensity. IEF values remained elevated but started to decline as the solar wind conditions normalized. Solar wind speeds remained high but started to decrease as the storm progressed.

The geomagnetic storm was associated with a significant coronal mass ejection (CME) and a high-speed solar wind stream from a coronal hole. These solar events contributed to the intense geomagnetic activity observed. The geomagnetic storm from November 6 to November 10, 2004, was a major space weather event characterized by severe geomagnetic activity. The significant drop in Dst, persistent southward IMF Bz, elevated IEF, and high solar wind speeds all contributed to the storm's intensity. This event resulted in dramatic auroras, potential disruptions to technology, and increased understanding of space weather impacts.

5.4. Event 3: The Geomagnetic Storm of March 7-11, 2012

The event of the geomagnetic storm on March 7-12, 2012 was also explained with the value of disturbance storm time (Dst) index top panel, interplanetary magnetic field

(IMF) (Bz) upper middle panel, interplanetary electric field (IEF) lower middle panel, and solar wind speed (SWS) bottom panel. For consecutive days plotted from March 7-2012 to 11-2012

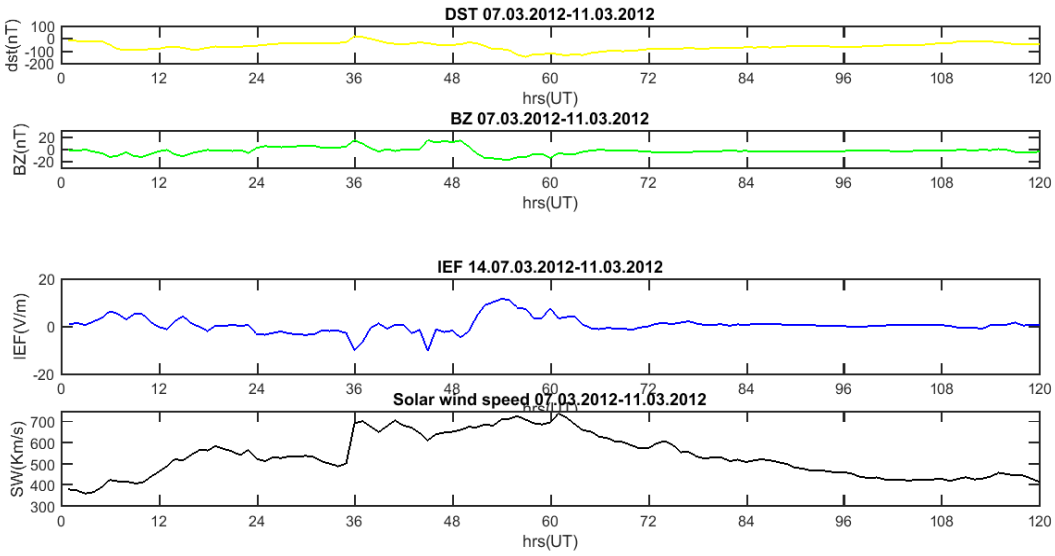

Figure 5.6 Dst index (top panel), IMF, Bz (upper middle panel), Solar wind speed (bottom panel), IEF (lower middle panel) during March 7-11, 2012

The initial phase of the storm started on March 7 and 8, with a Dst-index value of -88 nT at 09:00 UT and -53 nT at 22:00 UT, respectively. However, the main phase of the storm occurred on March 9; its value was -145 nT at 08:00 UT, which means the minimum Dst index value and the maximum geomagnetic storm were shown, and the maximum geomagnetic storm was categorized as an intense storm. This type of storm is associated with CME. Also the IMF (Bz), which shows southward on days 7 and 8, continuously started to oscillate between south and north directions. IEF values began to rise as solar wind conditions intensified and its solar wind speeds were elevated, around 500-600 km/s. At approximately 09-2012, the Bz component of the interplanetary magnetic field started to rotate towards a more magnetically connected polarity. Bz continued to be negative for several hours, reaching values near -17 nT, and its IEF reached elevated levels, contributing to the increased geomagnetic activity with an approximate solar wind speed of over 700 km/second. The Dst-index value increased, and the recovery storm started on March 10 and 11, with their corresponding Dst-index values of -81 nT at 02:00 UT and -64 nT at 24:00 UT. The storm type was a moderate storm for both. IMF Bz

continued to show negative values but began to fluctuate and move towards neutral or slightly positive. The IEF remained high but showed a gradual decline as the storm subsided. Solar wind speeds began to decrease, with values around 500-600 km/s.

The interplanetary electric field also shows fluctuations in an oscillatory manner. From Fig.5.6, there is a good interaction between the interplanetary magnetic field (IMF (Bz)) and the interplanetary electric field (IEF) because when the IMF is southward (negative), the IEF is positive (northward), which means that they move in opposite directions. Due to this, the charged particle easily enters the magnetosphere and is a good opportunity to reduce the Earth's magnetic field.

5.5. Event 4: The Geomagnetic Storm of March 15-19, 2015

Fig.(5.7) represents plots of disturbance storm time (Dst)index top panel interplanetary magnetic field IMF (Bz) upper middle panel, interplanetary electric field (IEF) lower middle panel and solar wind speed (SWS) bottom panel for five Consecutive days from day march 15th to 19th 2015 The initial phase of the storm day started from March 15 and 16, their Dst-index value -12 nT at 03:00 UT and -10 nT at 07:00 UT, the type of storm for initial phase categorized as minor (weak) storm. The storm was initiated on March 17, 2015, and its minimum Dst value is recorded at about -234 nT which reveals the storm is a great storm.

The Dst-index value increased and the recovery storm started on March 18 and 19 their corresponding Dst-index value was -200 nT at 24:00 UT and -99 nT at 24:00 UT respectively and an intense and moderate storm type was observed. The IMF was predominantly southward, with Bz values frequently dipping below -10 nT during the peak of the storm. This orientation enhanced magnetic reconnection with Earth’s magnetosphere. The IEF was elevated during the storm, particularly on March 16 and 17, due to the strong southward IMF, contributing to the overall geomagnetic intensity.

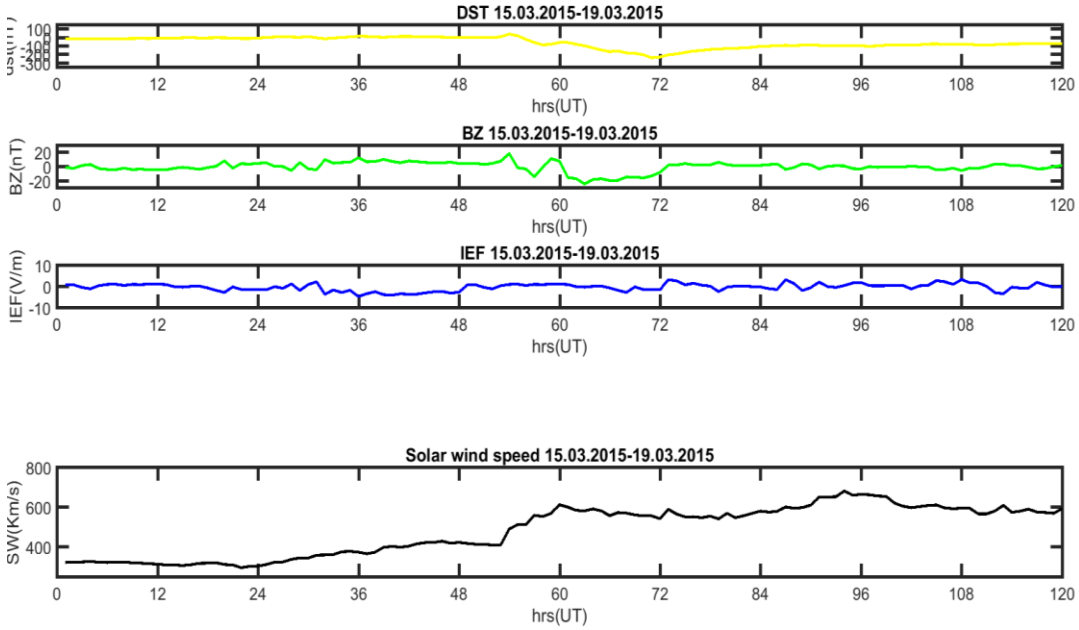

Figure 5.7: Dst index (top panel), IMF, Bz (upper middle panel), Solar wind speed (bottom panel), IEF (lower middle panel) during March 15-19 2015

The geomagnetic storms from March 15 to 19, 2015, were characterized by significant decreases in the Dst index, strong southward IMF, elevated IEF, and increased solar wind speeds. These conditions led to notable auroras and impacts on technological systems, highlighting the importance of understanding and monitoring space weather events.

5.6. Event 5: The Geomagnetic Storm of August 24-28, 2018

Figure. 5.8 represents plots of disturbance storm time (Dst) index top panel. Interplanetary magnetic field IMF (Bz) upper middle panel, interplanetary electric field (IEF) lower middle panel, and solar wind speed (SWS) bottom panel for five consecutive days from day plotted from August 24-2018 to August 28-2018. On August 24, initial disturbances began, with moderate increases in solar wind speed. Dst values started to decline, indicating the onset of geomagnetic activity, with Dst-index values of -13 nT at 15:00 UT and -50 nT at 23:00 UT. August 25: A significant increase in solar wind speed was recorded. The IMF turned predominantly southward, leading to stronger magnetic field interactions.

The type of storm for the initial phase was categorized as quiet and weak, respectively. The storm was initiated on August 26, 2018, and its minimum Dst value is recorded at

about -176 nT, which reveals the storm is an intense storm. The southward component of the IMF was particularly strong, with Bz frequently dropping below -10 nT, facilitating enhanced energy transfer into the magnetosphere. The IEF was elevated, especially during the storm peak, contributing to strong electric field effects in the magnetosphere.

The Dst-index value increased, and the recovery storm started on August 27 and 28; their corresponding Dst-index values were -72 nT at 07:00 UT and -47 nT at 24:00 UT, respectively. We observed a moderate and weak storm type.

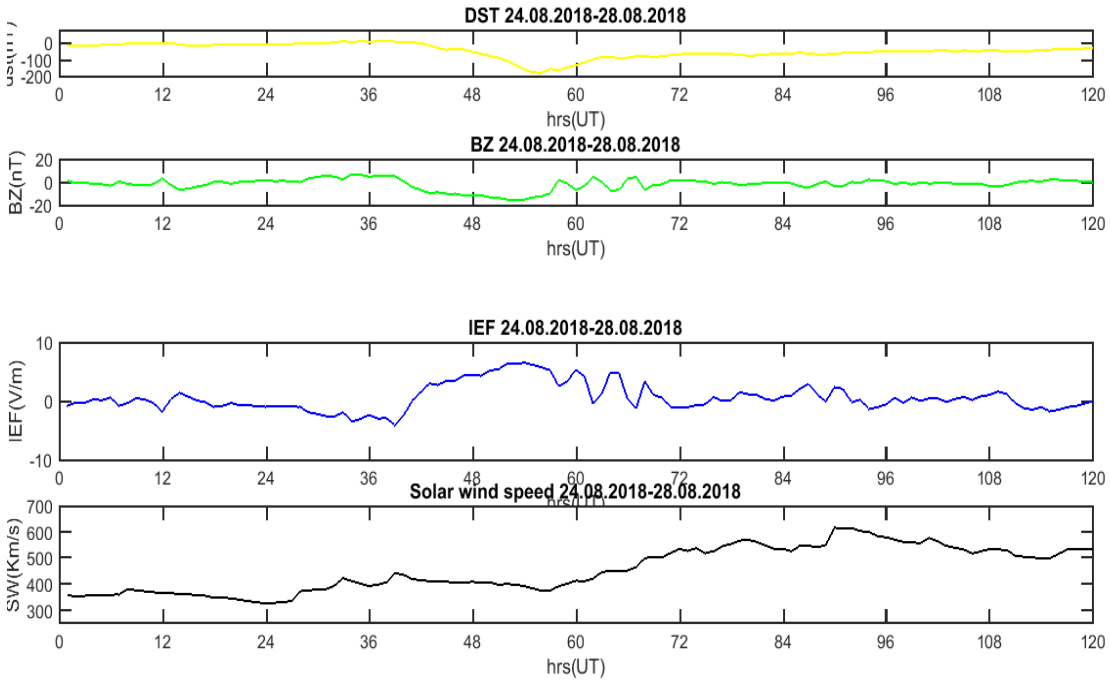

Figure 5.8: Dst index (top panel), IMF, Bz (upper middle panel), Solar wind speed (bottom panel), IEF (lower middle panel) during August 24-28 2018

As observed from Fig. 5.8, the IMF (Bz) is negative (southward) and the IEF northward (positive), so it decreased the ring current. But the solar wind speed positively increases, so the compression of the magnetosphere occurred.

The geomagnetic storms during this period were primarily caused by a combination of coronal hole high-speed streams (CH HSS) and potential coronal mass ejections (CMEs) that were observed in the solar wind. These solar phenomena released charged particles into space, which interacted with the Earth's magnetic field.

CHAPTER SIX

6. CONCLUSION AND RECOMMENDATION

6.1. Conclusion

The study of this thesis shows the comparison of geomagnetic storms from 1996 to 2019 of solar cycles 23 and 24. Geomagnetic storms are an important issue for the study of space weather. In this thesis, we study several solar wind parameters and geomagnetic indices. The Bz component is an important parameter that indicates the presence of a geomagnetic storm, and the yearly mean sunspot number for the years 1996 to 2007 varied from 12 to 174, while during the years 2008 to 2019, it was observed from 4 to 113. So on the basis of sunspot number, solar activity was noticeable during the years 1996 to 2007 in comparison to the years 2008 to 2019. In the years 2007–2009, there was a small number of sunspots, which was extremely low, and no major geomagnetic storm was recorded. The occurrence of geomagnetic storms during the years 1996-2007 (cycles 23) totalled 390 moderate, 83 intense, 15 great, and 7 super storms was observed, whereas during the years 2008–2019 (cycle 24), only 231 moderate, 34 intense, and 1 great storm were observed.

The present analysis also shows event 1, starting from July 14-2000 to July 18-2000, there was a large geomagnetic storm with a minimum value of -300 nT, and the source of the storm was CME. For event 2 from November 7-2004 to November 11-2004, the geomagnetic storm was also large, and the corresponding cause of the storm event was CME with a minimum value of -374 nT, whereas in the early phase of solar cycle 24, the most intense storm occurred during 07-08 March 2012; this storm Dst minimum reached -143 nT. The first great geomagnetic storm of solar cycle 24 did not occur until the declining phase on 17 March 2015, with its minimum value of -234 nT, and the source of the storm was the CME due to high solar activity. In short, the analysis shows that in cycle 23 events, 390 (78.95%) of the analysis show a moderate event, and the other 83 (16%) was an intense, 15 (3.036%) great storm, and 7 (1.41%) super storm event. In cycle 24, 231 (86.84%) show moderate, 34 (12.78%) are intense, and no great and super storm occurred.

Extended periods of southward IMF (Bz) lead to the main phase of the magnetic storm and are responsible for magnetic reconnection. On the other hand, northward IMF (Bz) has only minimal dayside reconnection. The increase in dayside reconnection increases the penetration of the solar wind into the magnetosphere; increases convection and ring current injection associated with high speed streams are smaller, and their Dst values are greater than (>-100 nT), whereas the storm caused by CME associated with high-speed and Dst value less than (<-100 nT), the magnetic field show high storm events and disturb the Earth magnetic field, which means that a higher negative value of the Dst index value causes reducing the Earth magnetic field and affects their purpose.

During solar cycles 23 and 24, geomagnetic storm intensity varied, with both cycles experiencing significant storms due to solar activity. Solar cycle 23 saw several intense storms, particularly in the early 2000s, while solar cycle 24 had fewer but still notable storms, with events in 2011 and 2012 being significant. The primary source of these storms was coronal mass ejection and, to a lesser extent, a high-speed solar wind stream.

6.2. Recommendations

Comparing geomagnetic storms across Solar Cycles 23 and 24 reveals important insights into the nature of solar activity and its effects on Earth. Understanding these differences can significantly enhance our predictive capabilities and readiness for future solar events. Continuous research and monitoring are essential to adapt to the evolving landscape of space weathers.

Bibliography

Arnold Hanslmeir, (2009) The sun and solar weather, university of Graz, Institute of physics/ IGAM, Australia 2nd

Brekke, A. (1997).*Physics of the upper polar atmosphere* (H. J. John Wiley, Ed.). Springer

Brekke, A., & Simmons, D. A. R. (1997).Physics of the upper polar atmosphere.*Polar Record*, **33**(1), 348-348. https://doi.org/10.1017/S0032247400020378

Burton, R. K., McPherron, R. L., & McIntosh, P. (1975).An empirical relationship between interplanetary magnetic field and Dst. *Geophysical Research Letters*, **80**(31), 4204-4214. https://doi.org/10.1029/GL080i031p04204

Davies, K. A. (1997).Studying the ionosphere with the Global Positioning System.*Radio Science*, **32**(1), 123-130. https://doi.org/10.1029/90RS00209

Davies, K. A., & Hartmann, G. K. (1990).Studying the ionosphere with the Global Positioning System.*Radio Science*, **32**(1), 123-130. https://doi.org/10.1029/90RS00209

Dungey, J. (1961).Interplanetary magnetic field and the auroral zones.*Physical Review Letters*, **6**(1), 47-49. https://doi.org/10.1103/PhysRevLett.6.47

Echer, E., de Souza, P. L., da Silva, A. B. C., & de Souza, M. A. S. (2008).Long-term correlation between solar and geomagnetic activity.*Journal of Atmospheric and Solar-Terrestrial Physics*, ***70***(11), 1638-1644. https://doi.org/10.1016/j.jastp.2008.05.002.

Feminella, F. S. (1997). Large-
scale dynamical phenomena during solar activity cycles.*Advances in Space Research*, **20**(7), 1303 -1306. https://doi.org/10.1016/S0273-1177(97)00676-6

Gonzalez, W. D., Tsurutani, B. T., & Gonzalez, A. L. C. (2007). Interplanetary conditions causing intense geomagnetic storms during solar cycle 23. *Geophysical Research Letters*, **34**(12), L12106. https://doi.org/10.1029/2007GL029202.

Gonzalez, W. G., (1990).Dual-peak solar cycle distribution of intense geomagnetic storms.*Planetary and Space Science*, **38**(2), 181-187.

Gonzalez, W. D., Gonzalez, A. L. C., & Tsurutani, B. T. (1990).Intense geomagnetic storms and their solar sources. *Planetary and Space Science*, **38**(2), 187-197. https://doi.org/10.1016/0032-0633(90)90149-I

Gopalswamy, N., (2014). Major solar events: A global perspective. *Earth, Planets and Space*, ***66***(1). https://doi.org/10.1186/s40645-014-0012-6

Gopalswamy, N. Y., (2010).Solar activity and its effects on the geosphere.*Sun and Geosphere*, **5**(7), 1-6.

Gopalswamy, N., Yashiro, S., & Akiyama, S. (2007). Characteristics of coronal mass ejections. *Journal of Geophysical Research*, **112**, A10. https://doi.org/10.1029/2007JA012123

Gummow, R.E. (2002). GIC effects on pipeline corrosion and corrosion control systems. *Corrosion Science*, **16**(64), 1755-1765. https://doi.org/10.1016/S0010-938X(02)00034-0

Hofmann-Wellenhof, B., Lichtenegger, H., & Collins, J. (2001).*Global positioning system: Theory and practice*. Springe.

Hargreaves, J. (1992).*The solar terrestrial environment: An introduction to the space environment*. Cambridge University Press.

Kane, R. (1997).Quasi-biennial and quasi-triennial oscillations in geomagnetic activity indices.*Annales Geophysicae*, ***15***(2), 267-272. https://doi.org/10.1007/s00585-997-0267-3

Kelley, M. C. (1989). *The Earth's ionosphere: Plasma physics and electrodynamics* International Geophysics Series, **Vol. 43**). Academic Press.

Mohannakumar,K,(2008). Startosphere, troposphere interaction: an introduction. Cochin India,springer.

Moldwin, M. (2008).An introduction to space weather.*Space Weather Journal*, **59**, 1800-1809. https://doi.org/10.1029/2008SW000410

Okeke, F. N., & Hamano, Y. (2000).Daily variations of geomagnetic H, D, and Z fields.*Earth, Planets and Space*, **52**(9), 841-846. https://doi.org/10.1186/BF03352714

Phillips, T., & Tony, S. (2013). The effects of space weather on aviation. *Journal of Aviation Technology and Engineering*, **2**(1), 1-7. https://doi.org/10.5703/1288284314636

Rees, H. (1994).*Physics of the upper atmosphere* (**Vol. II**).Cambridge University Press.

Rishbeth, H., & Garriott, O. (1969).*Introduction to ionospheric physics* (1st ed.). Academic Press

Schunk, R. W., & Nagy, A. F. (2009).*Ionosphere physics and chemistry* (2nd ed.). Cambridge University Press.

Scott, J. W. (2007).Modelling the temporal variation of the ionosphere in a network.*Journal of Atmospheric and Solar-Terrestrial Physics*, *69*(**8**), 1026-1037. https://doi.org/10.1016/j.jastp.2007.02.003

Yu, Y., You, W., Wang, X., & Qiu, B. (2009).A global ionospheric perturbation.*Chinese Journal of Geophysics*, *52*(**1**), 1-12. https://doi.org/10.1002/cjg2.181